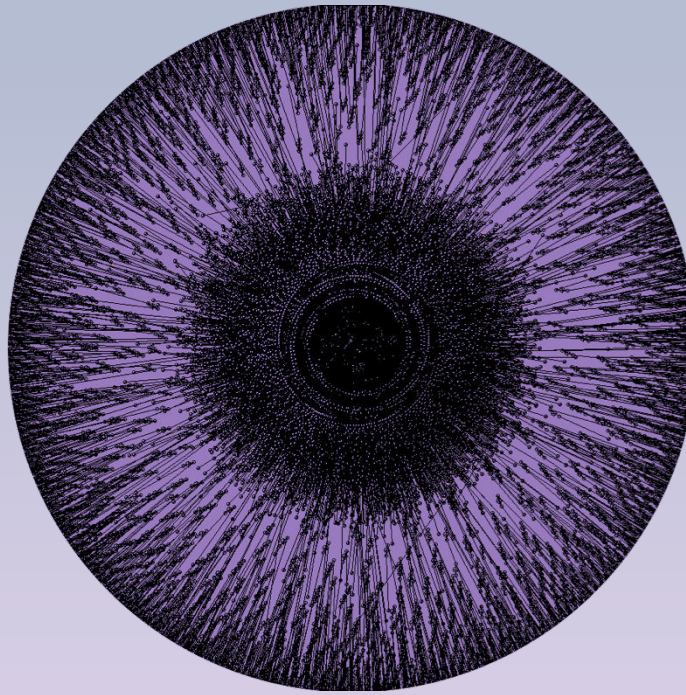


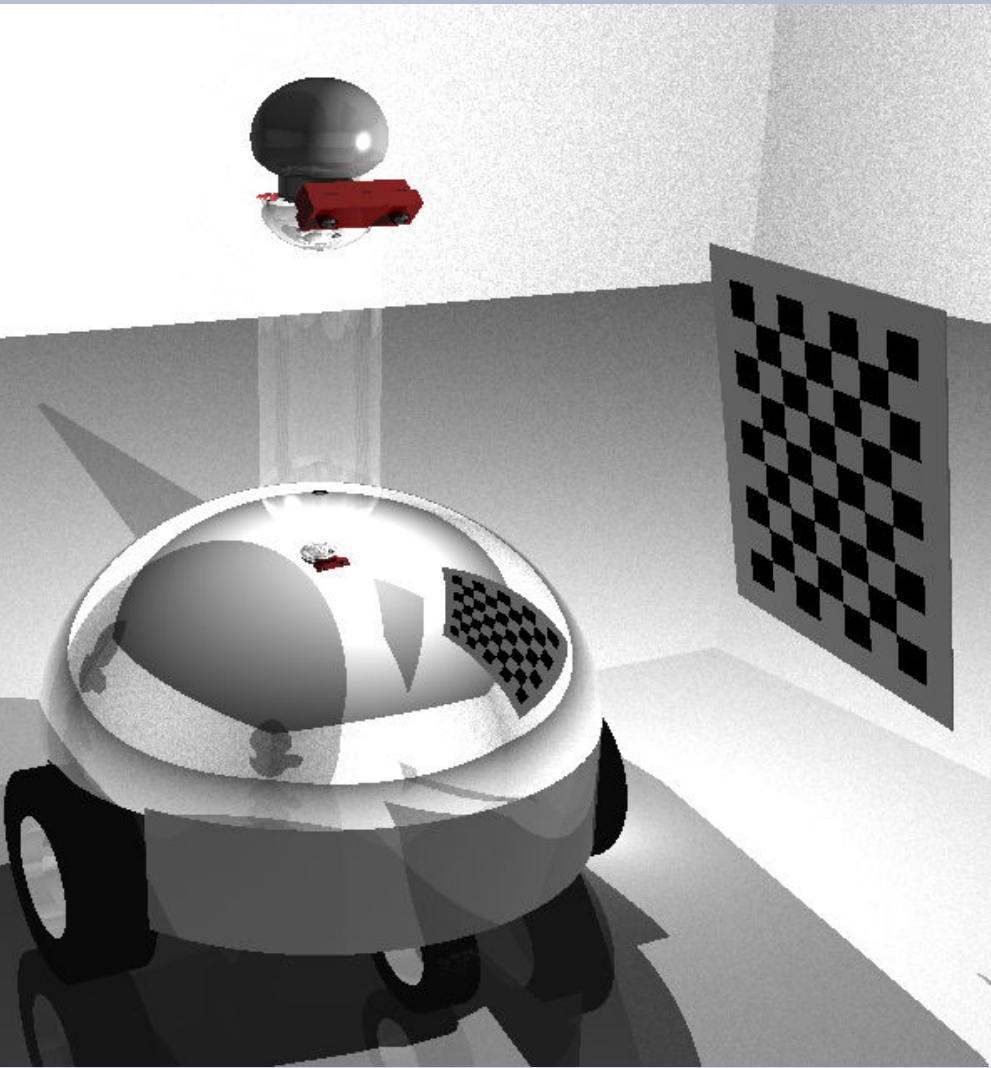
Fusing Optical Flow and Stereo in a Spherical Depth Panorama Using a Single-Camera Folded Catadioptric Rig



Igor Labutov, Carlos Jaramillo & Jizhong Xiao

Robotics Lab
City College of New York
ICRA 2011

Presentation Outline



POV-Ray Robot Model

- Introduction
- Rig Design (Model)
- Omnidirectional Stereo Geometry (*Sphereo*)
- Depth from Omnidirectional Optical Flow
 - 3-D De-rotation
- Fusion of the 2 Modalities
- Results and Conclusion

Introduction > Rig Design > Stereo Geometry > Optical Flow > Fusion > Results and Conclusion

Introduction

- 3-D world = Surround Vision
- Eye geometry of insects

360° azimuthal field of view.

- Catadioptric Sensors

Catoptrics (Mirror) + Dioptic (Lenses)

- Guiding Visual

- Guiding Robots

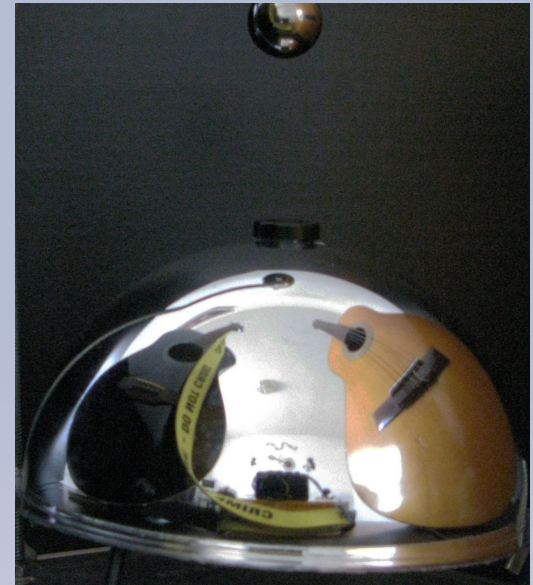
Omnidirectional

- Aerial

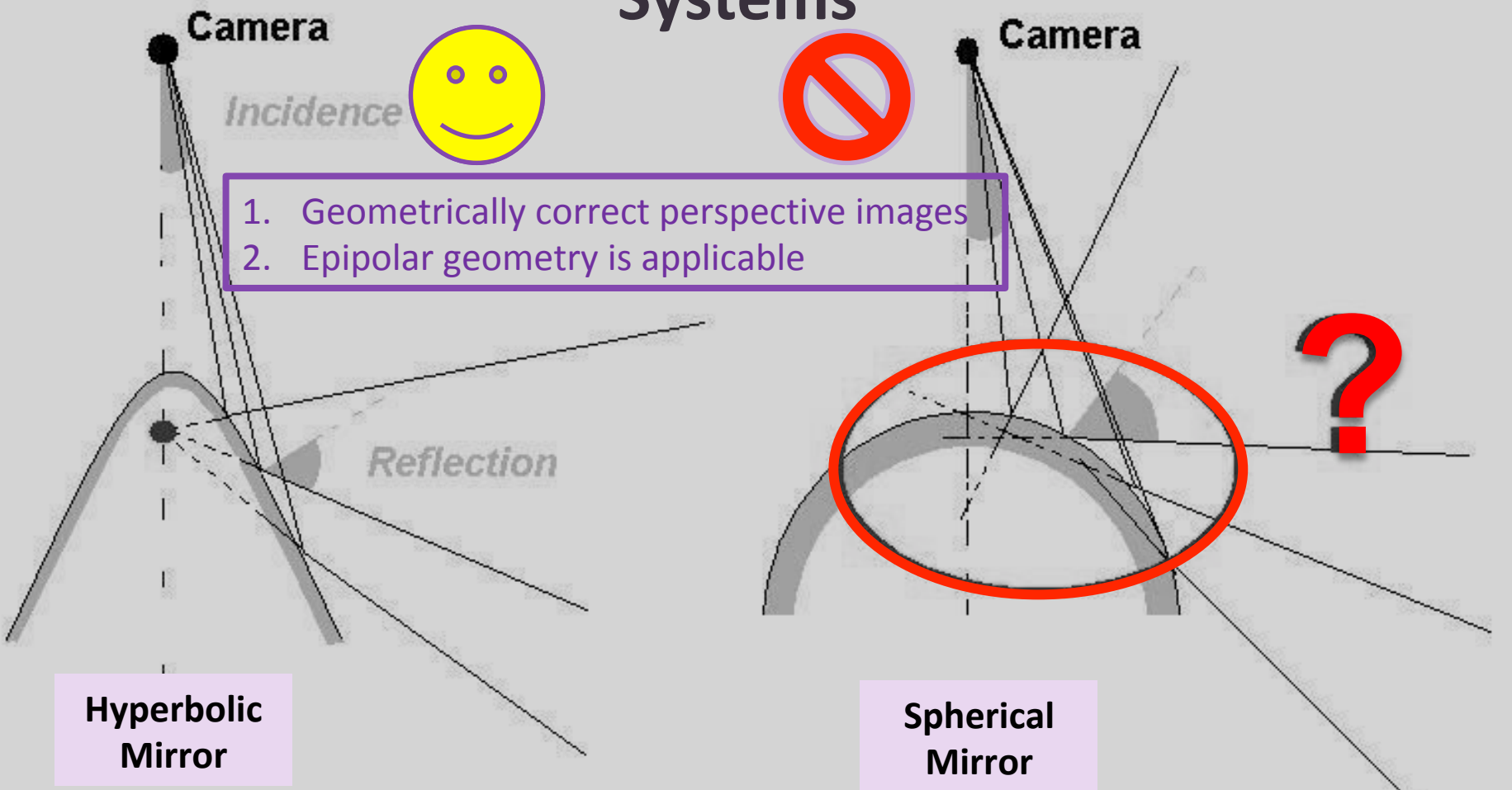


Introduction > Rig Design > Stereo Geometry > Optical Flow > Fusion > Results and Conclusion

- **Coaxial Alignment:**
Standard monocular web-camera
+
2 spherical mirrors???
- **Spherical Mirrors Cons:**
 - No Single ViewPoint (SVP)



SVP constraint = Only with Central Projection Systems



[Introduction](#) > Rig Design > Stereo Geometry > Optical Flow > Fusion > Results and Conclusion

- **Coaxial Alignment:**

Standard monocular web-camera

+

2 spherical mirrors???

- **Spherical Mirrors Cons:**

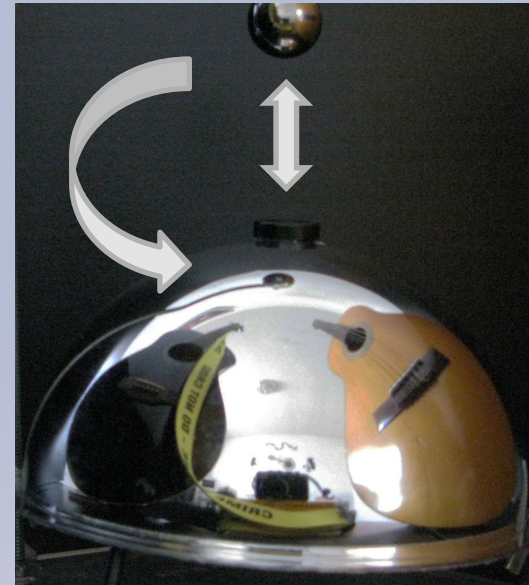
- No Single ViewPoint (SVP)
- Lower resolution + Higher distortion (true for all mirrors)

- **Spherical Mirrors Pros:**

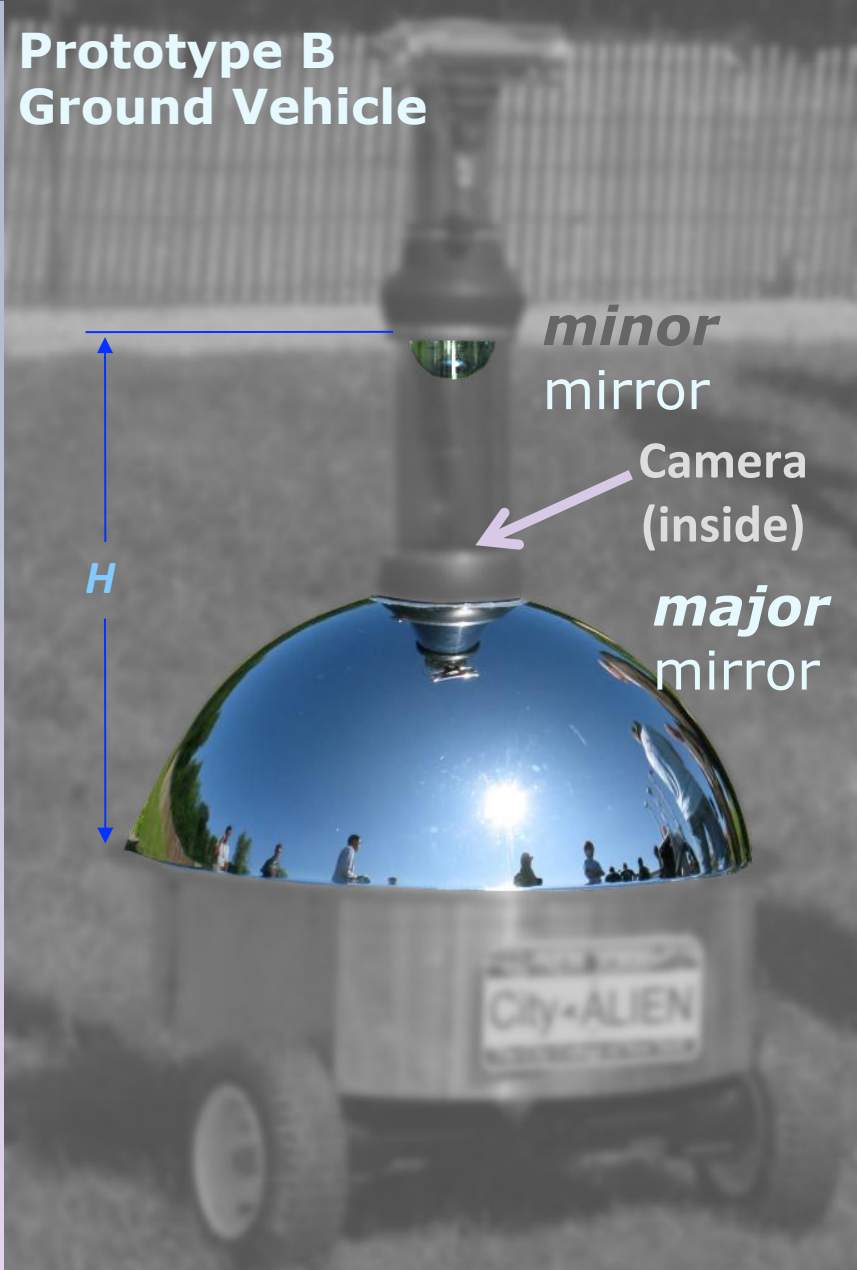
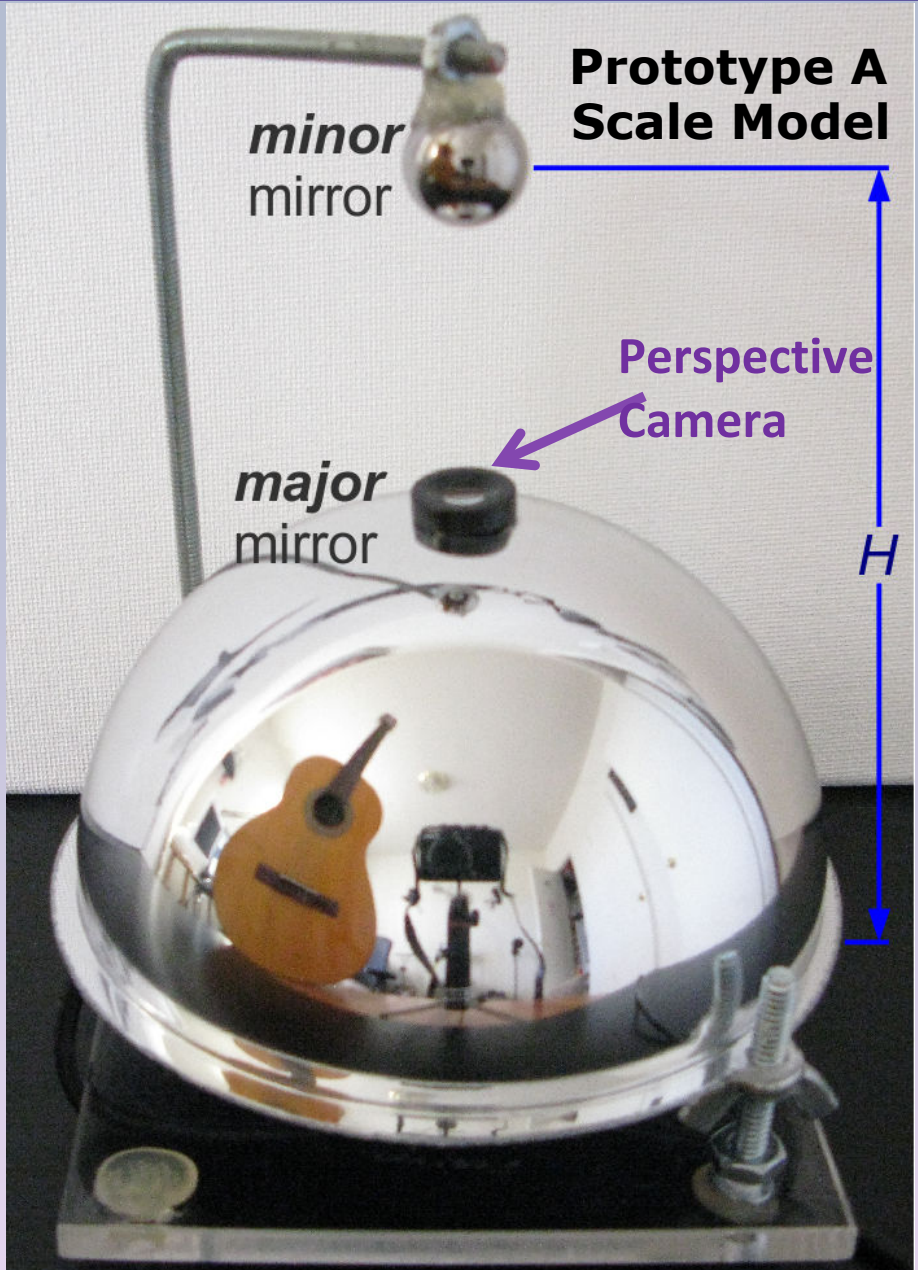
- **Cheaper** to build and **low weight**
- No multi-calibration issues (1 single camera to calibrate)
- No synchronization problems + **No misalignments**

Introduction > Rig Design > Stereo Geometry > Optical Flow > Fusion > Results and Conclusion

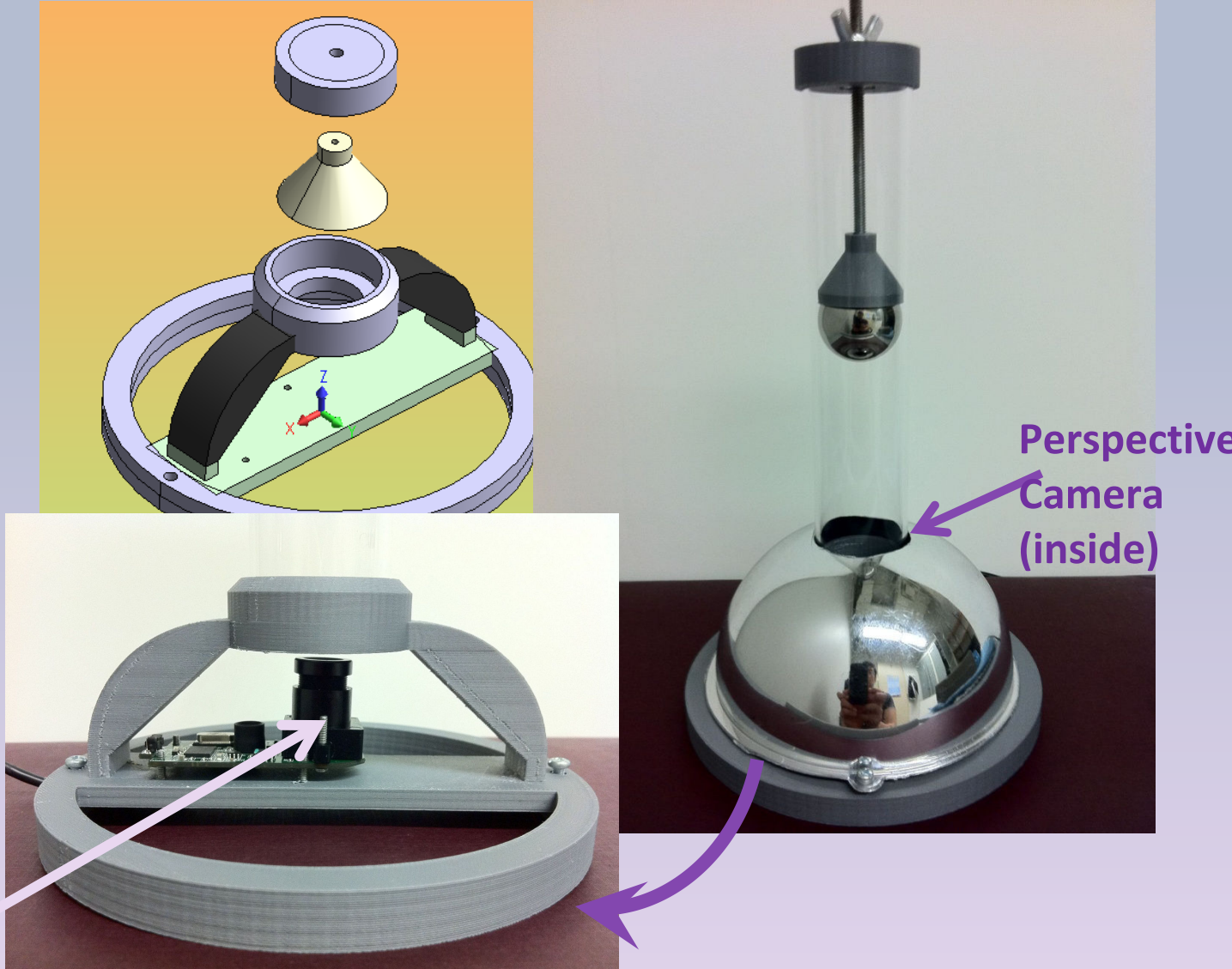
○ **Larger vertical FOV**



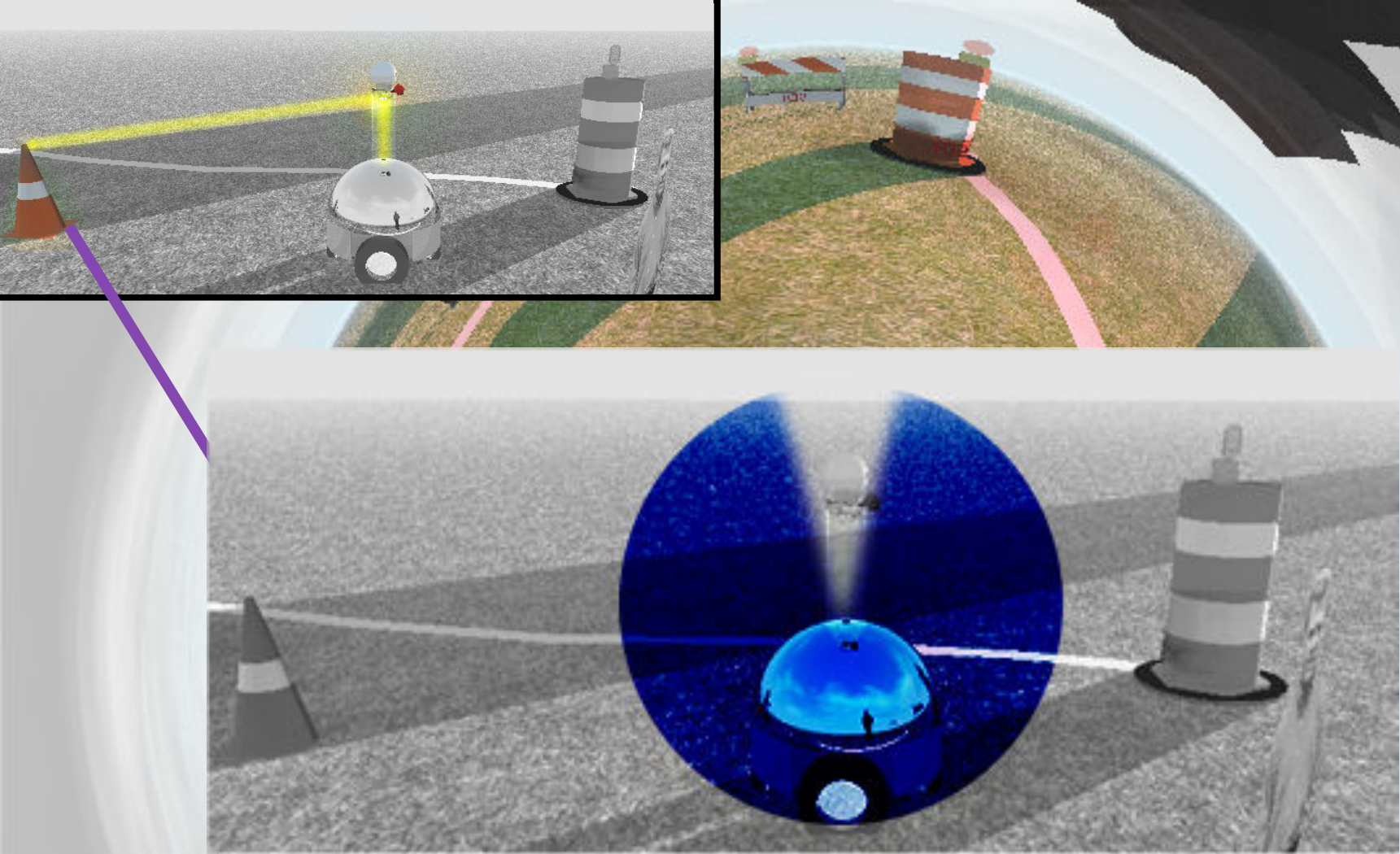
Folded-Configuration Models



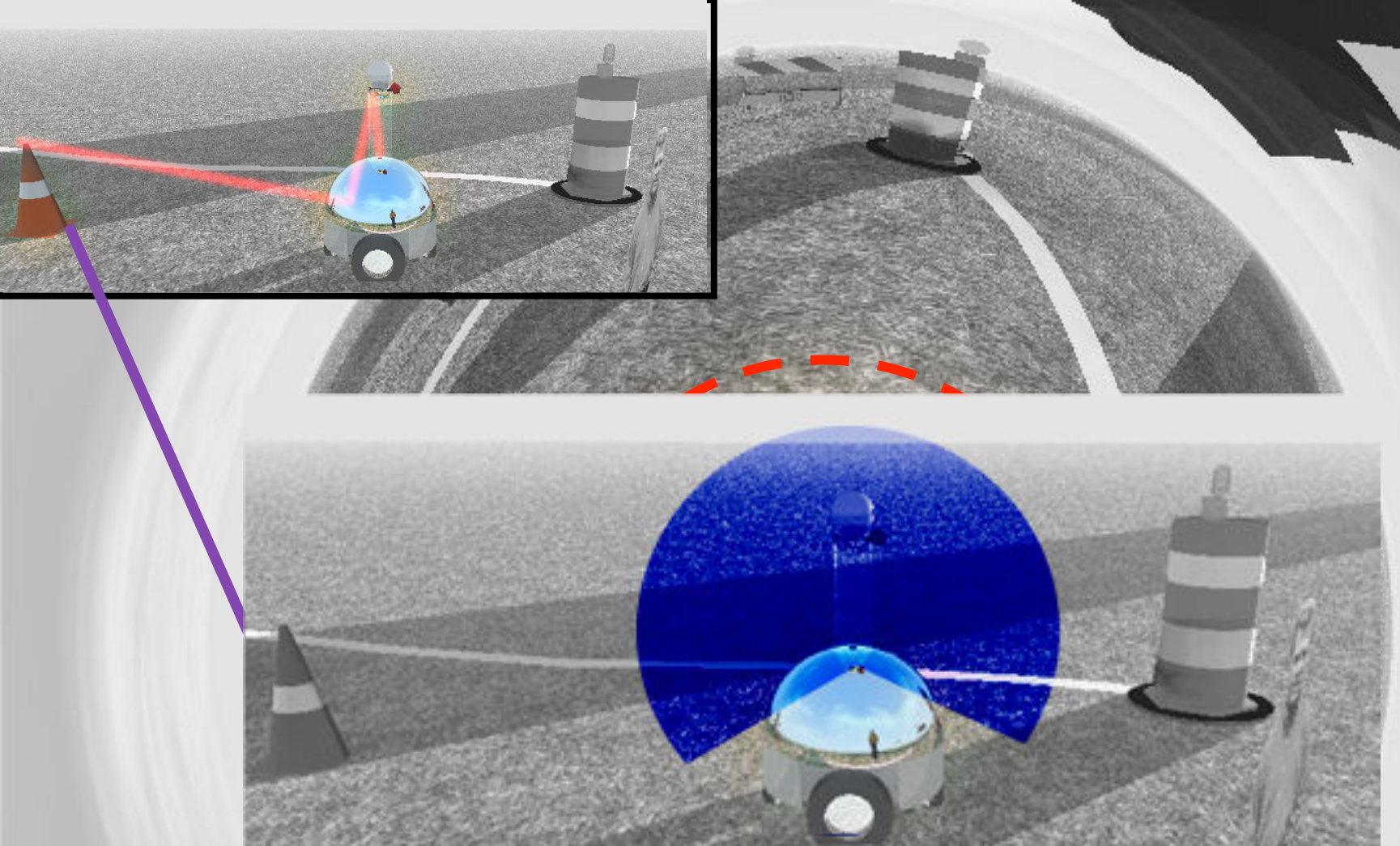
Folded-Configuration Models



Introduction > **Rig Design** > Stereo Geometry > Optical Flow > Fusion > Results and Conclusion

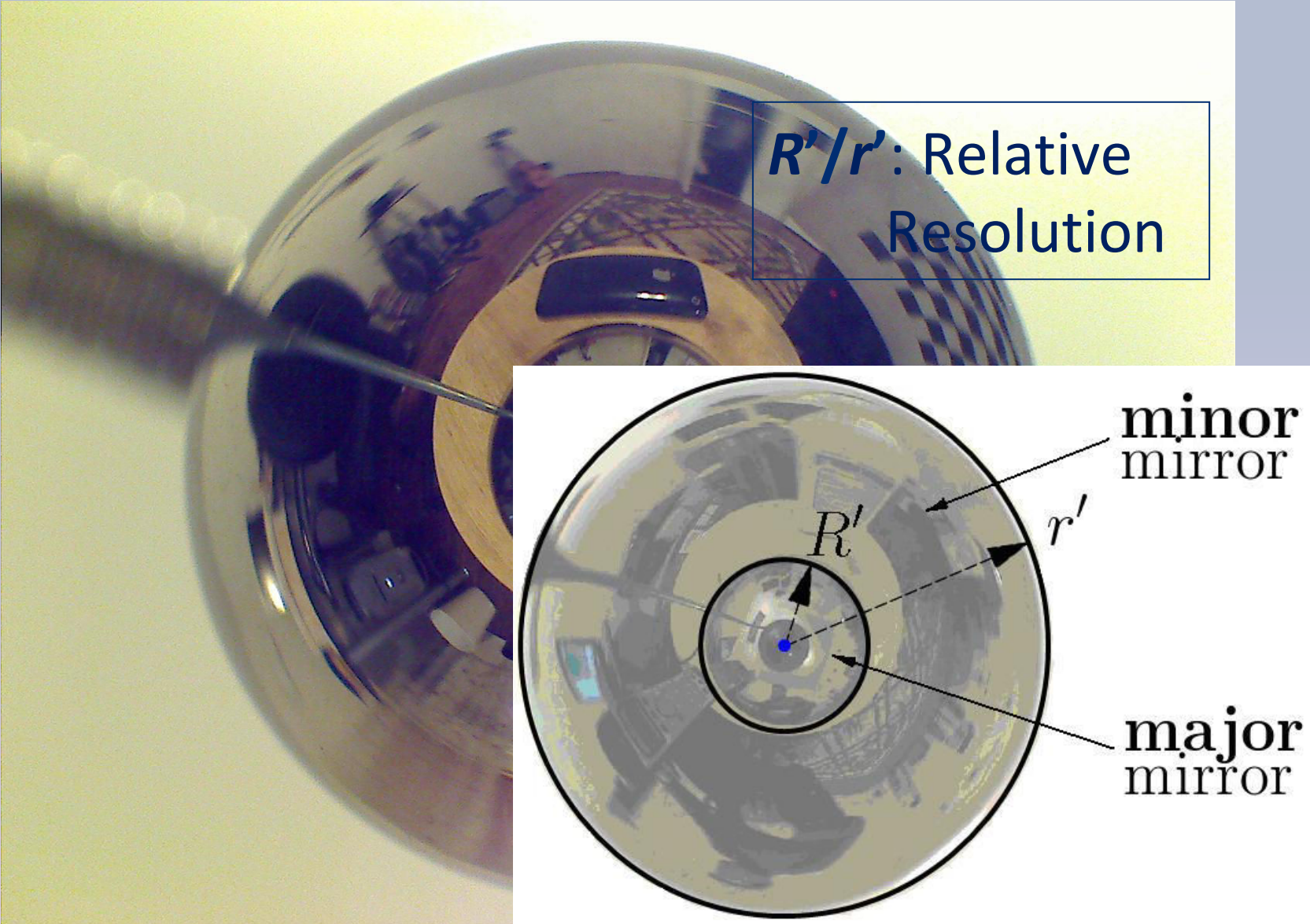


Minor Mirror mostly images the ground



Major Mirror mostly images the sky

Image Acquisition



Introduction > **Rig Design** > Stereo Geometry > Optical Flow > Fusion > Results and Conclusion

Design Parameters

- Assumptions

- Single Viewpoint
- FOV of camera F is $< 2\beta$

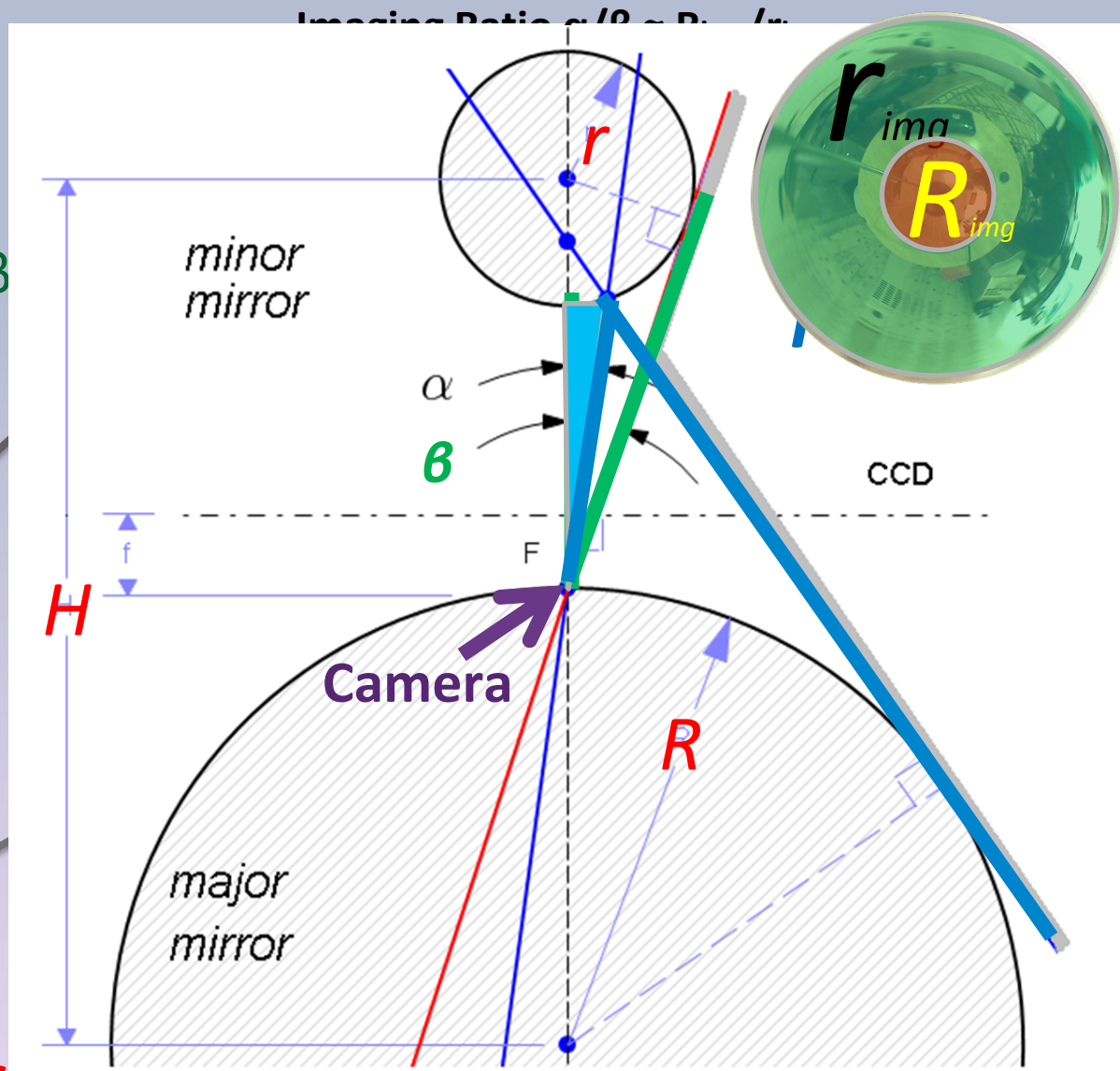
- Linearization Constraints

$$H \gg r \quad \text{and} \quad R \gg r$$

$$\frac{R_{img}}{r_{img}} \approx \frac{\alpha}{\beta} = \frac{R}{H\sqrt{2}}$$

$$FOV = \pi - \frac{R}{H}$$

Less than 10% deviation
when $H > 2R$ and $R > 2r$



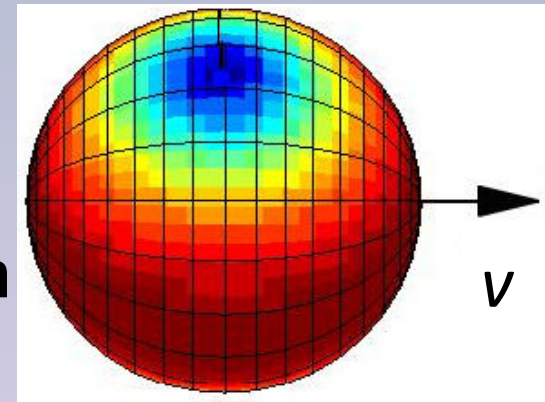
Modality 1: SPHEREO (Stereo Vision with Mirror Spheres)

- Has been attempted MANY times
- **Problem:**
Depth may be recovered only in a **NARROW** (<30 degrees) **band** around the equator of the view-sphere

Modality 2: **OPTICAL FLOW** = Visual Features + Motion

Has been attempted too!

Problem 1 - Provides depth everywhere except in the direction of your own motion



Problem 2 - Only RELATIVE depth
(Scale Factor needed)

Problem 3 - Needs motion!!!

Introduction > Rig Design > Stereo Geometry > Optical Flow > Fusion > Results and Conclusion

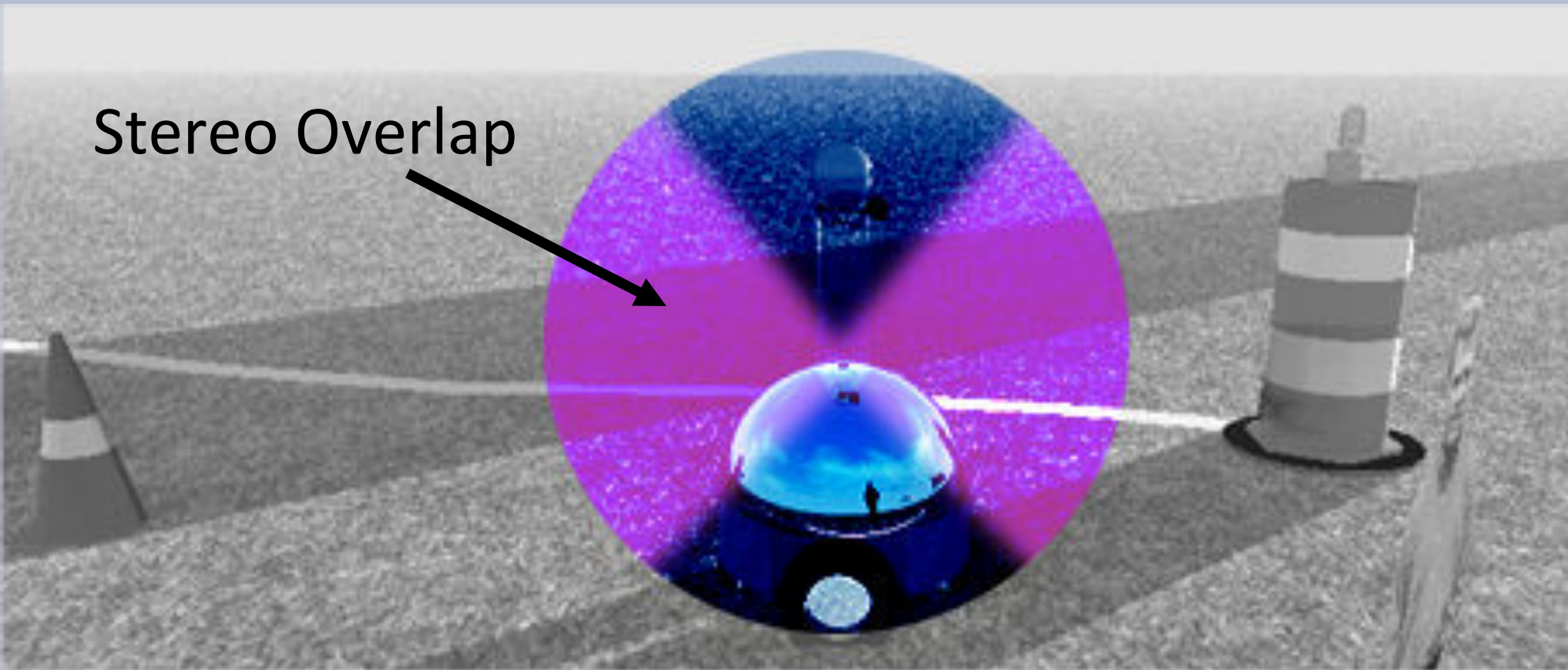
SPHEREO + OPTICAL FLOW

Has NOT been attempted in catadioptrics

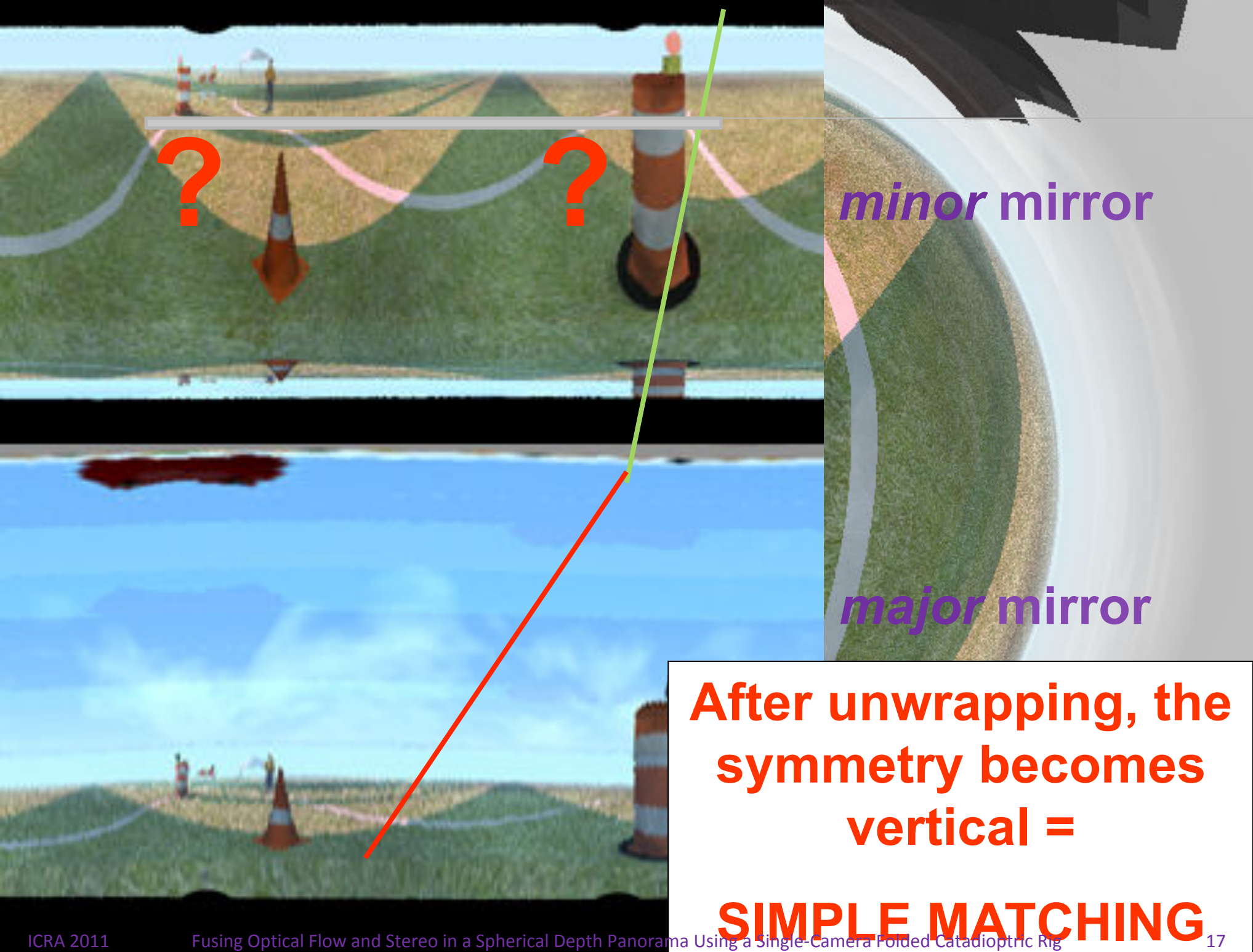
Goal: To take advantage of 2 Modalities:

- * **Stereo:** higher resolution on equator
- * **Optical Flow:** better around poles
=> **Fusion** solves problem of relativism (**scale factor**) of depth from Optical Flow

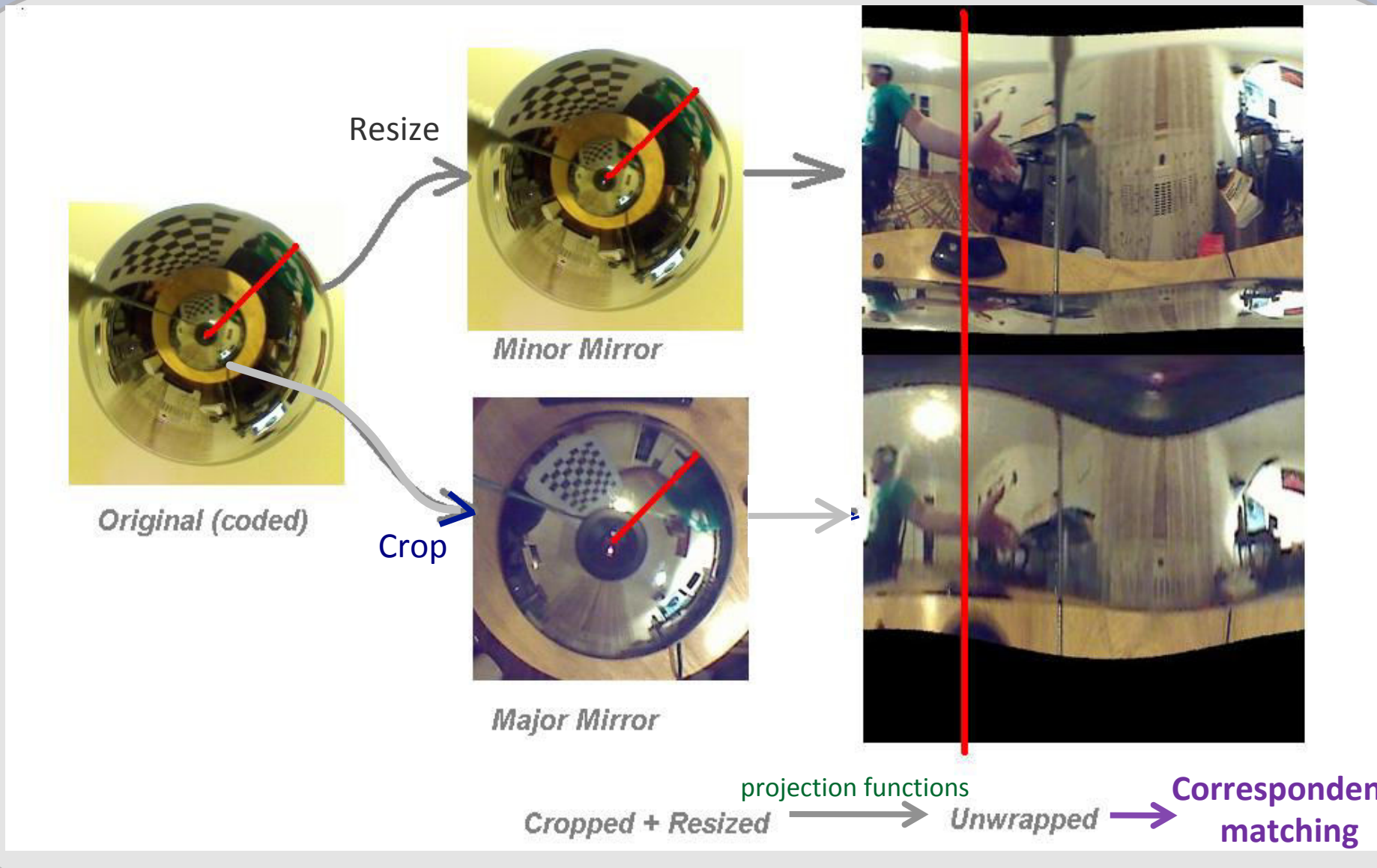
Omnidirectional Sphereo



Introduction > Rig Design > **Stereo Geometry** > Optical Flow > Fusion > Results and Conclusion



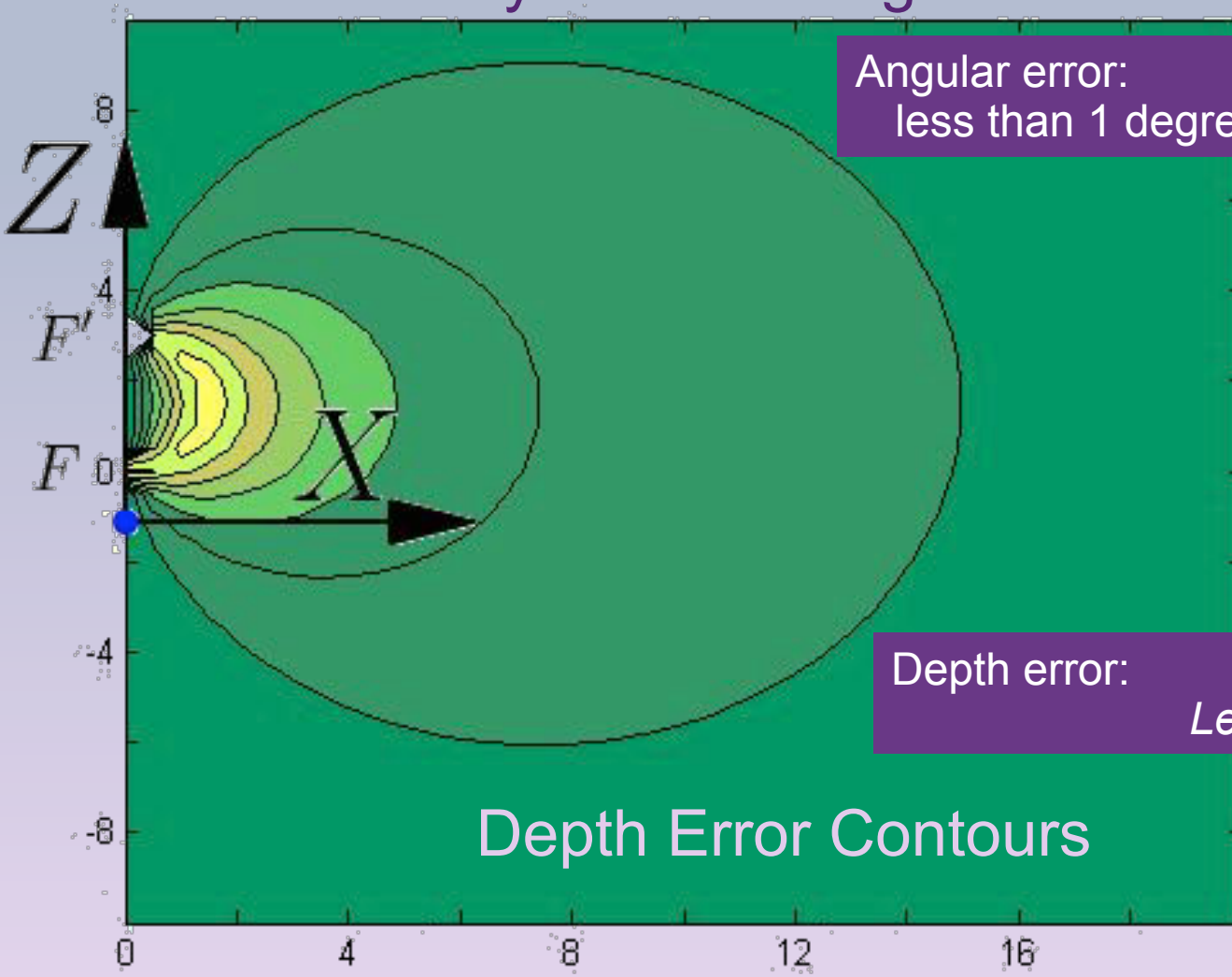
Stereo Pipeline



Introduction > Rig Design > **Stereo Geometry** > Optical Flow > Fusion > Results and Conclusion

Triangulation Uncertainty

Derivative of projection function $f(u)$ goes to infinity near the edges.



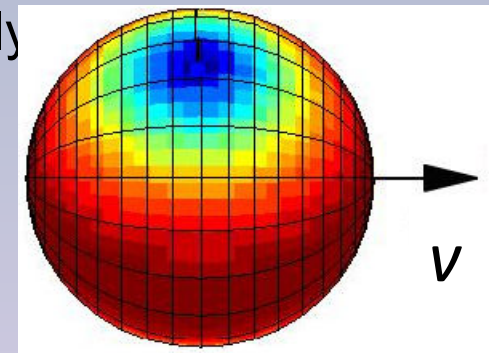
Introduction > Rig Design > **Stereo Geometry** > Optical Flow > Fusion > Results and Conclusion

ADVANTAGES:

For *horizontal motion* (e.g.), strongest optical flow occurs ABOVE and BELOW the rig

+ Compensates for STEREO which is mostly best near the EQUATOR

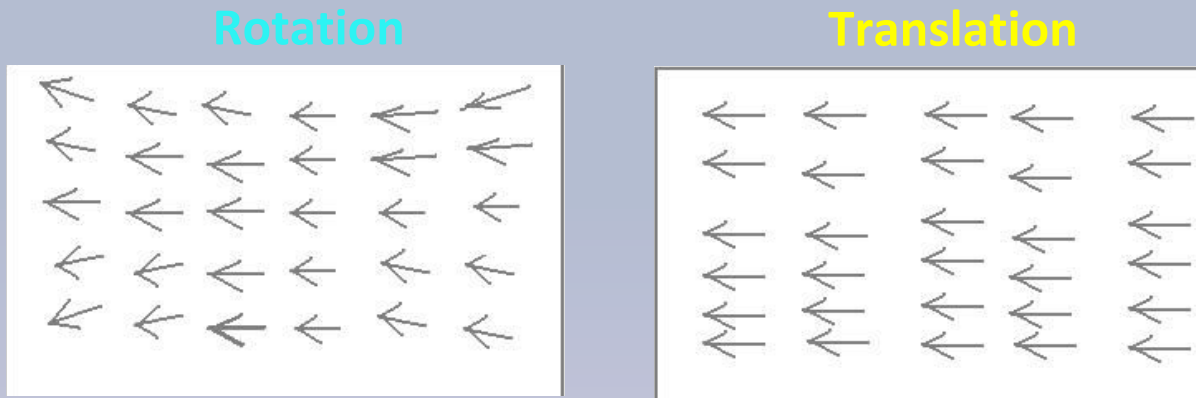
...BUT **2** DISADVANTAGES:



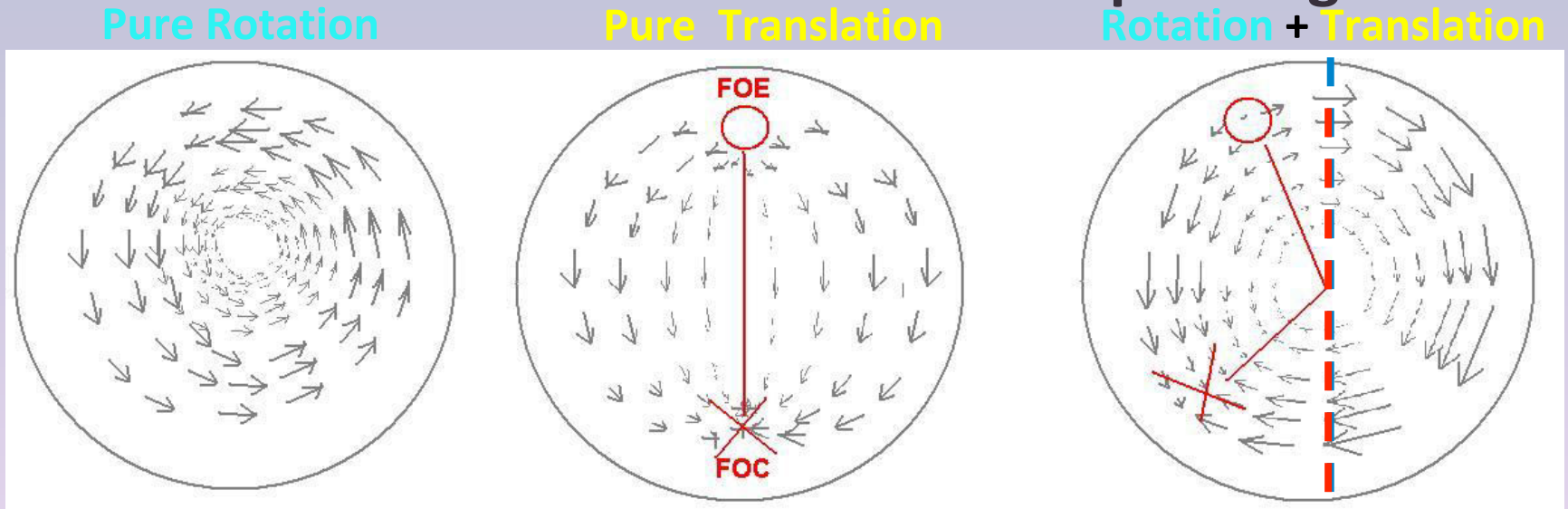
1. Optical Flow field **must be de-rotated** first
2. Depth can **only** be recovered up to scale factor

De-Rotation of Optical Flow

- De-rotation with single (narrow field-of-view) camera:



- De-rotation with Omnidirectional Catadioptric Rig

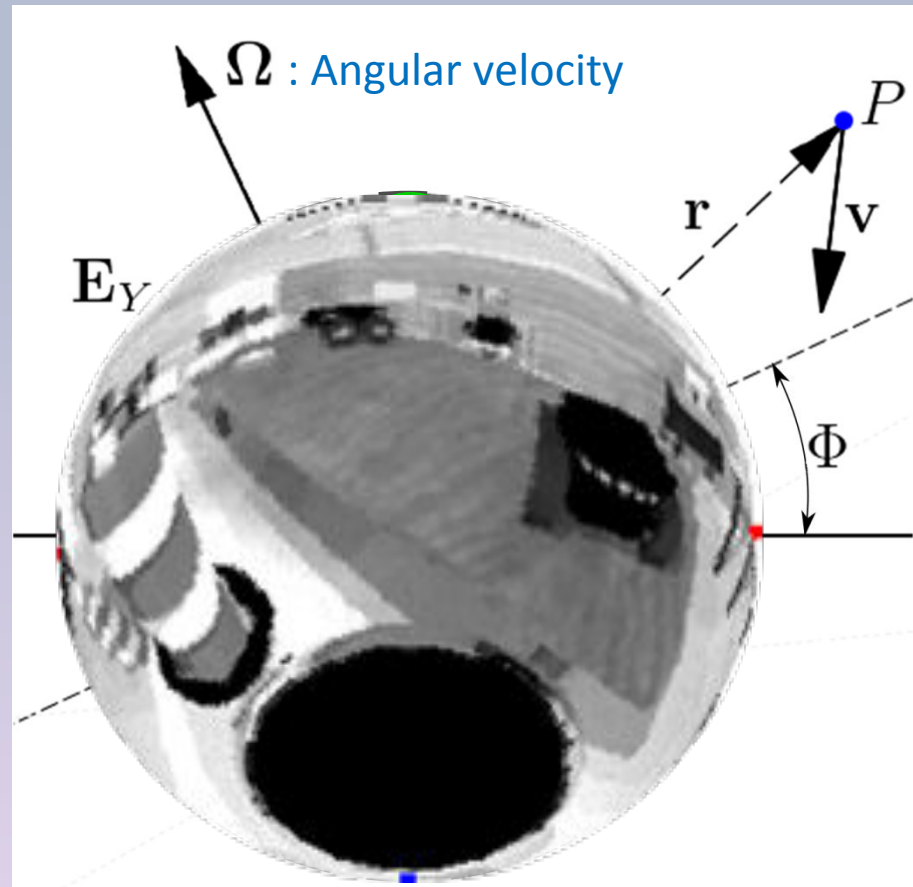


Introduction > Rig Design > Stereo Geometry > **Optical Flow** > Fusion > Results and Conclusion

De-rotation (cont.)

DE-ROTATION of omnidirectional images has only been attempted* onto a plane using **Nelson-Aloimonos Algorithm**

- exploits the distinct global rotational and translational flow patterns
- recover components using a simple **2D search** along ANY three great circles (**E_x, E_y, E_z**)



*C. McCarthy, N. Barnes, and M. Srinivasan, "Real time biologically-inspired depth maps from spherical flow," 2007 IEEE International Conference on Robotics and Automation, 2007,

De-rotation (cont.)

Projection bands (e_x , e_y , e_z) of the 3 Great circles:

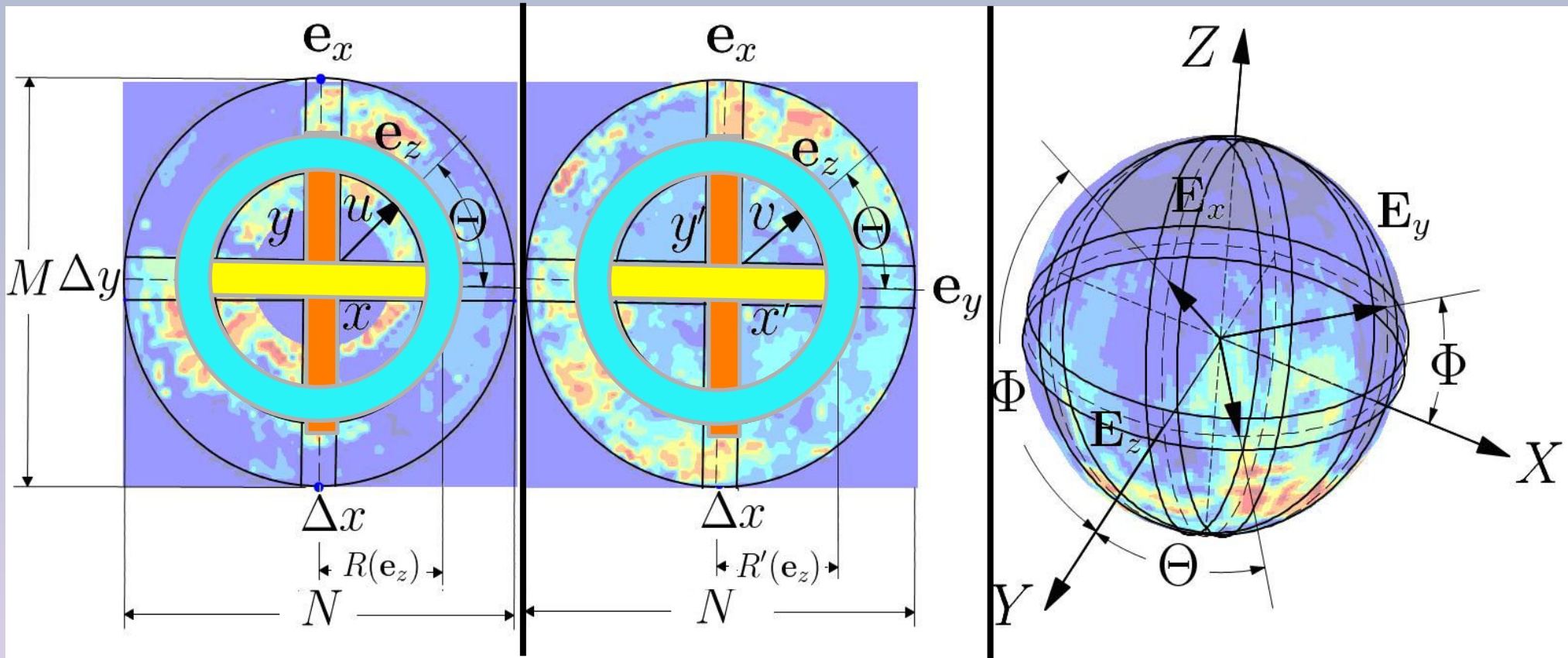


Image of *minor* mirror

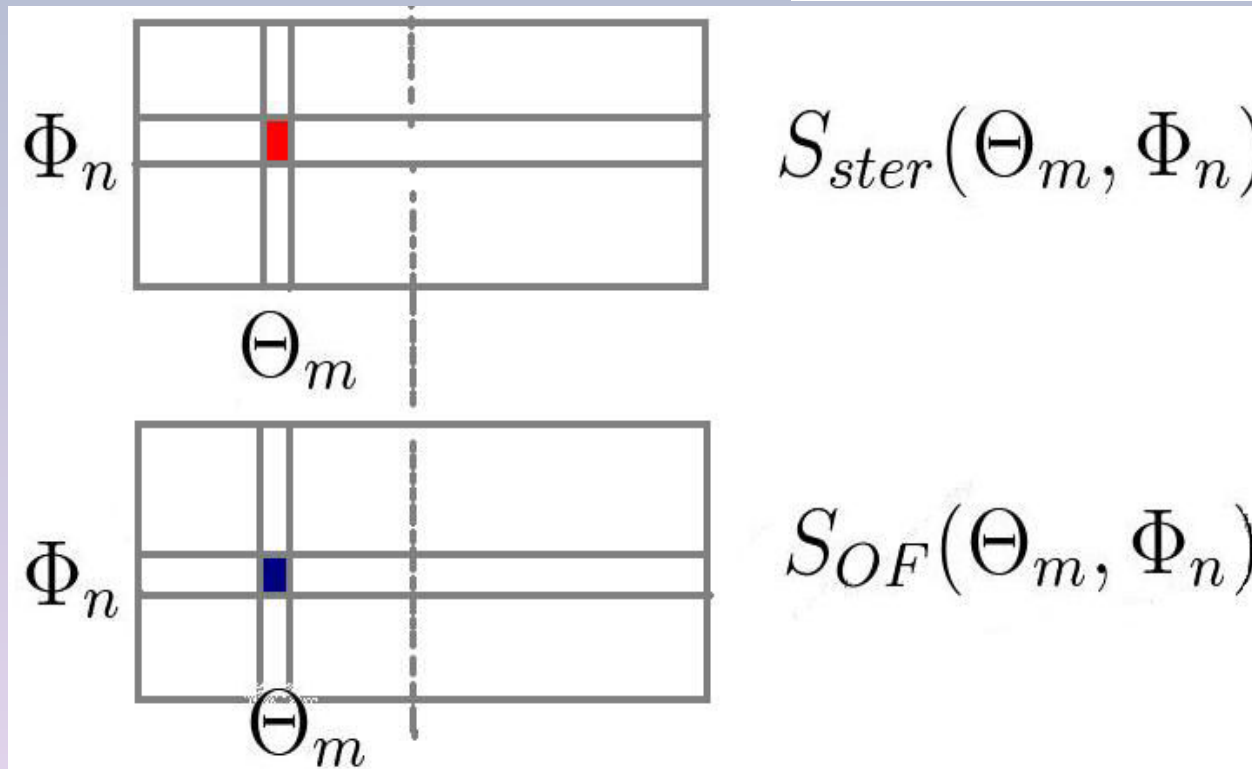
Image of *major* mirror

Images projected onto
Viewsphere

Minimization with Weighted Least Squared on overlaps

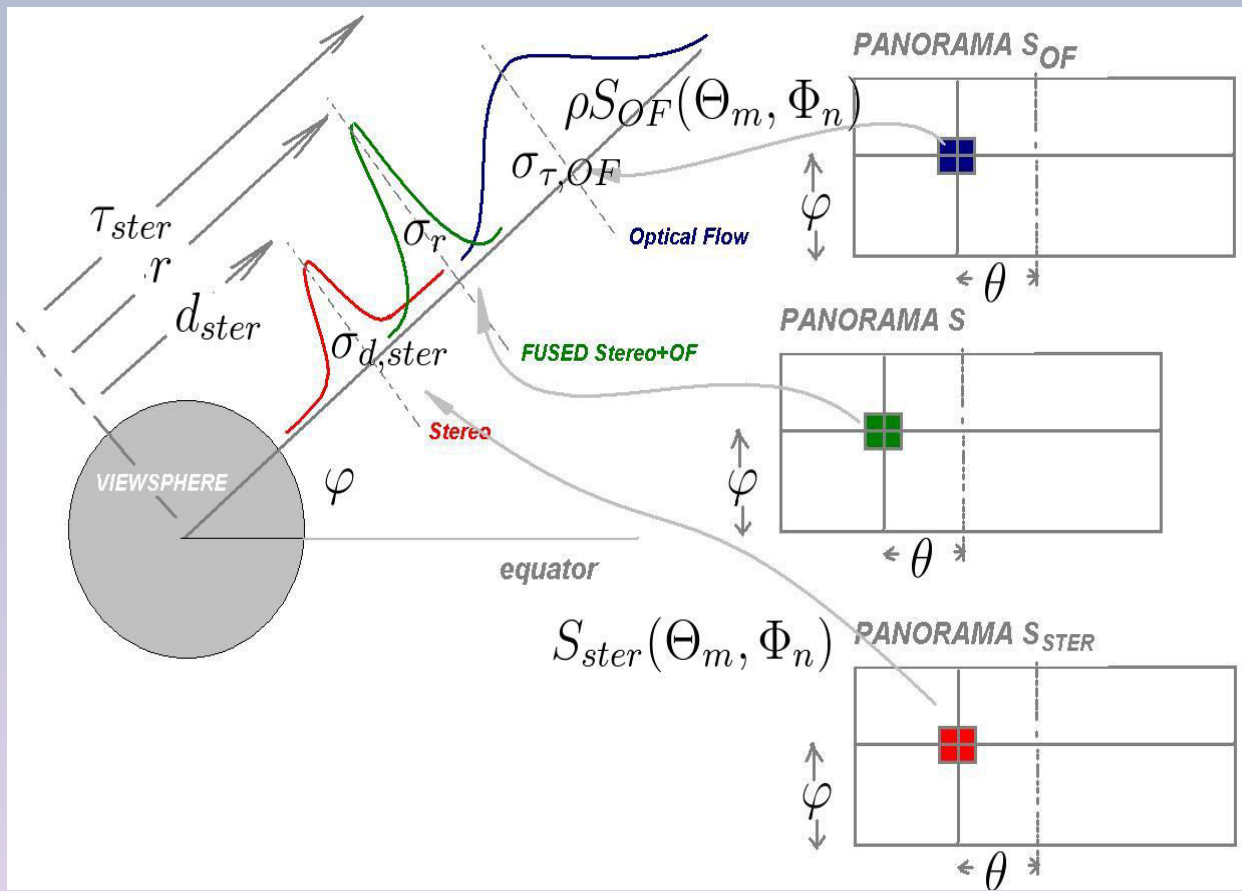
$$\rho = \arg \min_{\rho} \sum_{\Theta_m}^M \sum_{\Phi_n}^N d_{\Theta_m, \Phi_n}^2(\rho)$$

$$d_{\Theta_m, \Phi_n} = \frac{S_{ster}(\Theta_m, \Phi_n) - \rho S_{OF}(\Theta_m, \Phi_n)}{\sigma_{ster}^2(\Theta_m, \Phi_n) \sigma_{OF}^2(\Theta_m, \Phi_n)}$$



Introduction > Rig Design > Stereo Geometry > **Optical Flow** > Fusion > Results and Conclusion

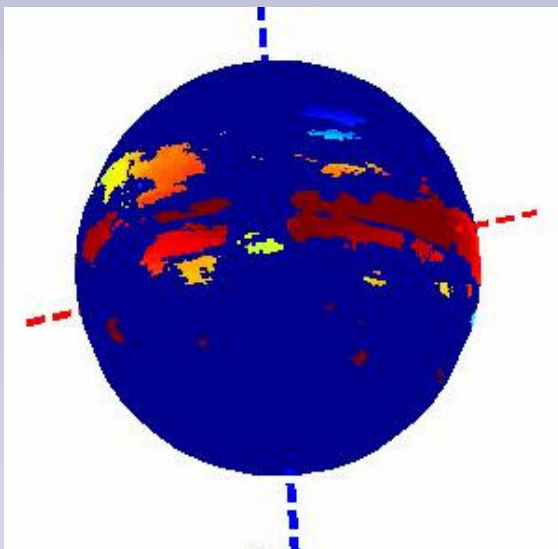
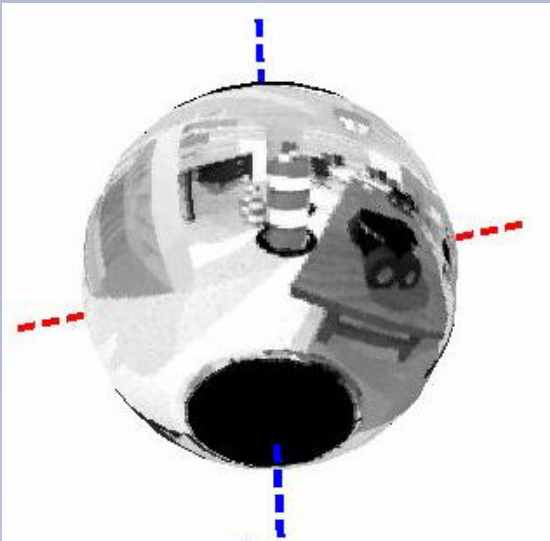
Performed in a panoramic image S
using standard **linear sensor fusion equations**



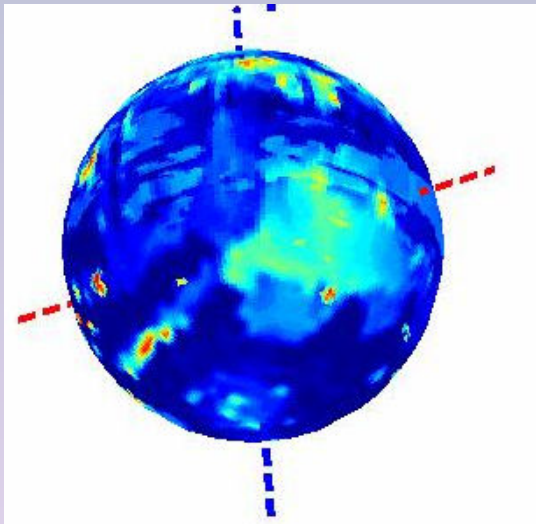
$$r = \frac{d_{ster} \sigma_{\tau, OF}^2 + \tau_{OF} \rho^2 \sigma_{d, ster}^2}{\sigma_{d, ster}^2 + \rho^2 \sigma_{\tau, OF}^2}$$

$$\sigma_r^2 = \frac{1}{\sigma_{d, ster}^{-2} + \rho^{-2} \sigma_{\tau, OF}^{-2}}$$

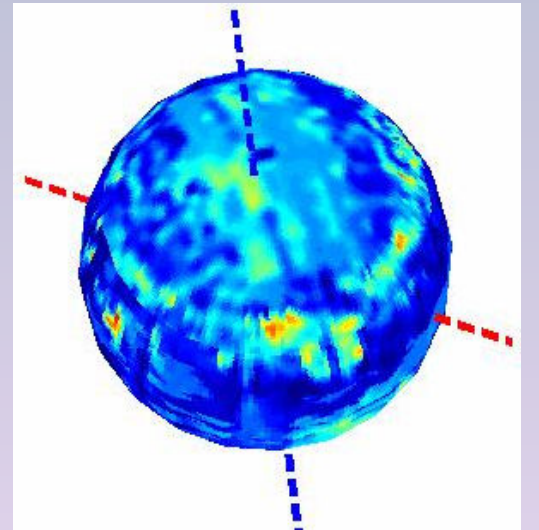
Experiments - Simulations



Disparity Panorama



Disp+OF Panorama (S)



Disp+OF Panorama (N)

Introduction > Rig Design > Stereo Geometry > Optical Flow > Fusion > **Results and Conclusion**

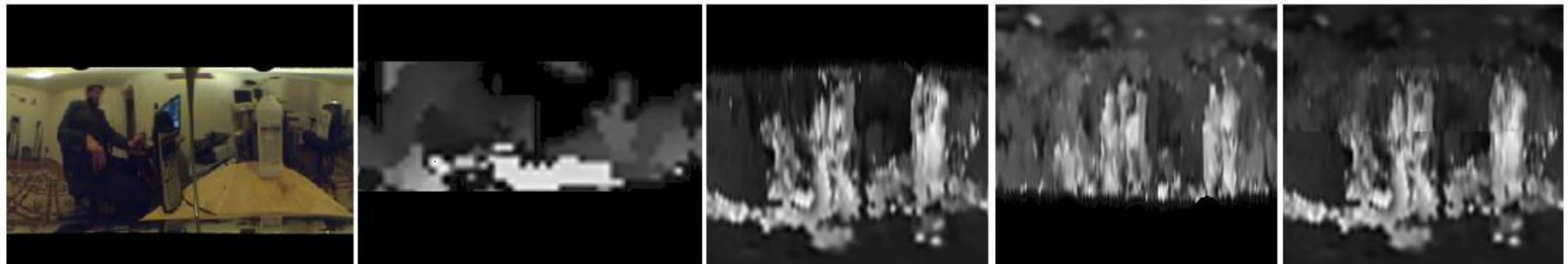
Experiments – Real World

Major Pan

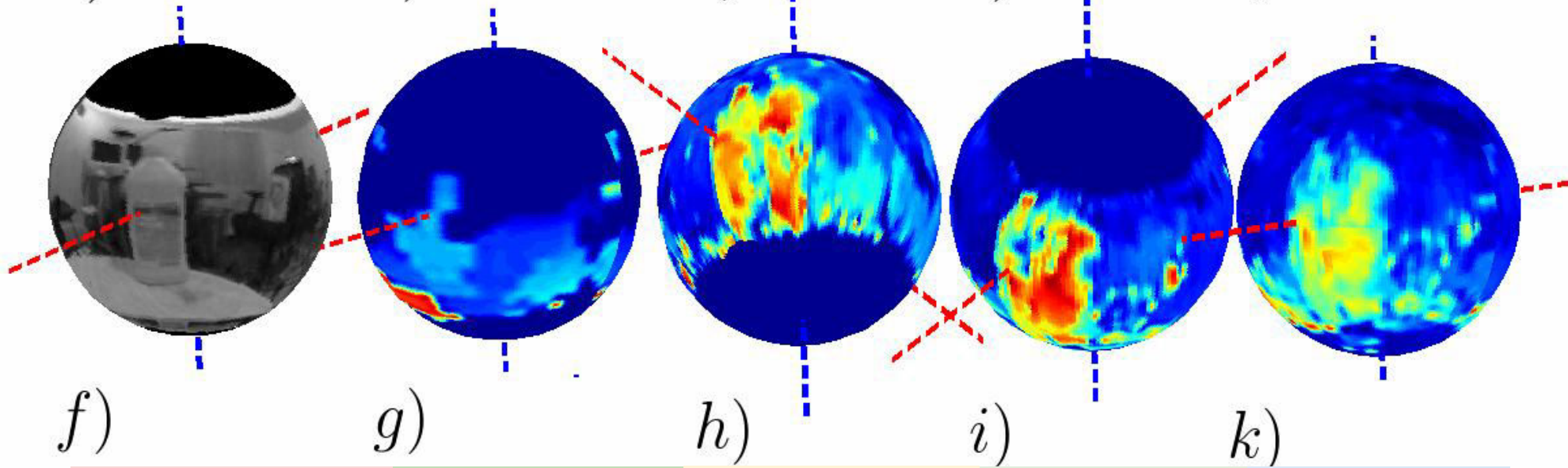
Stereo

SOF from F

fused S



a) b) c) d) e)



projections of (a,b,c,d,e) on the view-sphere

Introduction > Rig Design > Stereo Geometry > Optical Flow > Fusion > **Results and Conclusion**

Summary of Contribution

1. We use spherical mirrors in a folded configuration to maximize image resolution near the poles of the viewsphere.
 - For robots moving in a horizontal plane, this generates high-resolution relative depth from optical flow above and below the robot.
2. We exploit radial epipolar geometry of the spherical mirrors to compute dense metric-depth in the equatorial region of the view-sphere.
3. We fuse depth from optical-flow (poles) and stereo (equator) in a dense probabilistic depth panorama to obtain comparable depth resolution in every direction.
 - The scale factor for depth-from-optical-flow is recovered by using weighted least-squares in regions where depth from optical flow and stereo overlap.

Introduction > Rig Design > Stereo Geometry > Optical Flow > Fusion > **Results and Conclusion**

Remarks and Future Work

- Theoretically demonstrated with off-line imagery
- The fusion of these two modalities (stereo and optical flow) can generate an almost-entire view-sphere of probabilistic range information
- Exceptions are self-occluded areas on the poles.
- Greater errors in areas where neither modality provides sufficient depth resolution (no-overlapping regions and near the edges → high distortion and low resolution).

FUTURE:

- Deeper analysis of uncertainty in each modality
- Real-time performance of the system.
 - Try sparse optical flow (feature correspondences) with the Nelson-Aloimonos' de-rotation algorithm.

Introduction > Rig Design > Stereo Geometry > Optical Flow > Fusion > **Results and Conclusion**

Acknowledgement

The work is supported in part by:



**National Science Foundation (NSF) under
grant No. ECS-0421159, CNS-0424539,
CNS-0551598, CNS-0619577, IIS-0644127**

and



**U.S. Army Research Office (ARO) under
grant No. W911NF-05-1-0011,
W911NF-09-1-0565**

Thank you!

